RAPID COMMUNICATIONS

PHYSICAL REVIEW B VOLUME 46, NUMBER 7 15 AUGUST 1992-I

Local bonding structure of deuterium in single-crystal silicon determined by nuclear magnetic resonance

J. B. Boyce, N. M. Johnson, S. E. Ready, and J. Walker
Xerox Palo Alto Research Center, Palo Alto, California 94304
(Received 17 March 1992)

Nuclear magnetic resonance was used to determine the local structure of deuterium in single-crystal silicon. The deuterium was introduced by hydrogenation and incorporated in hydrogen-induced extended planar defects. The spectrum consists of two components: a narrow doublet and a broad central line. The splitting and orientational dependence of the doublet establish that it arises from D bonded to Si with the Si-D bonds aligned along the ⟨111⟩ directions. The broad central line is similar to that observed in hydrogenated amorphous silicon and may arise from motionally inhibited D_2 in the dilated region of the hydrogen-induced platelets.

It has been established that hydrogen, diffused into single-crystal silicon (*c*-Si) at moderate temperatures (e.g., $\leq 250\,^{\circ}C$), can generate extended structural defects as well as passivate dopants, deep-level impurities, and native defects.[1] These hydrogen-induced extended defects are unrelated to either plasma or radiation damage and do not involve hydrogen decoration of either preexisting or plasma-induced defects.[2] Rather, it appears that isolated, interstitial hydrogen can, under certain conditions, generate hydrogen-stabilized defects in the silicon lattice. These defects are planar in shape, are aligned predominantly along {111} crystallographic planes, and involve the coordinated formation of Si-H bonds.[3,4] Platelet generation appears to involve the precipitation of a two-dimensional silicon hydride phase from a supersaturated solution of hydrogen in silicon.[5] Although several theoretical models have been proposed for platelets,[6–9] their microscopic structure has yet to be determined experimentally. These defects are of technological interest since similar extended defects have been observed after reactive ion etching of silicon wafers[10,11] and in low-temperature epitaxially grown silicon,[12] and H-Si bonding directly determines the electronic properties of hydrogenated amorphous silicon (*a*-Si:H).[13]

Nuclear magnetic resonance (NMR) is one of the most successful techniques for determining the local bonding structure of hydrogen in materials. Yet, up to now it has not been successfully applied to hydrogen in a single-crystal semiconductor due to severe sensitivity limitations. NMR requires a large total number of nuclear spins (typically corresponding to $> 1\times10^{18}$ cm^{-3}), while the solubility of hydrogen in a crystalline semiconductor is extremely low (e.g., $\sim 1\times10^{15}$ cm^{-3} at 1100 °C in *c*-Si) (Ref. 14) and standard hydrogenation techniques[3] introduce H in substantial (metastable) concentrations only near the exposed surface. One approach that can overcome the sensitivity limitation for surface incvestigations is to use finely powdered samples. However, this approach is unsatisfactory for studies of hydrogen in a bulk single-crystal environment because the crushing process introduces extensive damage within the individual particles that can dominate hydrogen incorporation.

We have overcome the sensitivity limitation and obtained atomic-scale information on the microscopic structure of hydrogen that is incorporated in platelets in single-crystal silicon, with deuterium substituted for hydrogen. The NMR spectrum consists of a two-component line: (1) a narrow doublet line and (2) a broad central, unsplit line. The doublet has a splitting characteristic of the Si-D bond, and its dependence on the orientation of the crystal with respect to the external magnetic field shows that this Si-D bond is aligned along the ⟨111⟩ directions, in agreement with the orientation of the platelets as seen in transmission electron microscopy (TEM).[1] The central NMR line is similar to that observed in *a*-Si:D where it has been attributed to D in strained bonds.[15] Such strained bonds also exist in hydrogenated *c*-Si, in the vicinity of the deuterium-induced platelets.[3] Another component of this central line could be molecular D_2. It is too broad to be freely rotating molecular D_2 but could consist of D_2 confined in voids in the crystal,[16] such as in the dilated regions of the platelets.

Two strategies were implemented to achieve a sufficient signal-to-noise ratio for the NMR measurement. First, deuterium was substituted for hydrogen since its lower natural abundance (0.0156%) reduces the background signal to a negligible level; D also provides an additional probe of the local environment via its quadrupole moment which is zero for H. Second, since platelets are generated only near the exposed surface, it was necessary to stack together a set of thin deuterated wafers to form a composite. The wafers were 3 mils thick, of (100) orientation, doped *n*-type (2×10^{18} P cm^{-3}), and polished on both surfaces. Both surfaces of each wafer were individually deuterated, in a remote plasma reactor,[3] with a two-step treatment[5] that maximized the areal density of platelets. A set of 76 such wafers, rectangular in shape (0.64×1.9 cm^2), with the ⟨110⟩ directions aligned with the edges of the rectangle, formed the NMR sample (total volume 0.68 cm^3).

The depth profile of deuterium in an NMR specimen is shown in Fig. 1 and was obtained by secondary-ion mass spectrometry (SIMS). The D concentration is high at the surface but falls off rapidly with depth to the background level at about 200 nm below the surface. The depth-integrated density of deuterium in platelets is 5.5×10^{15} cm^{-2}, with an absolute accuracy of the SIMS measure-

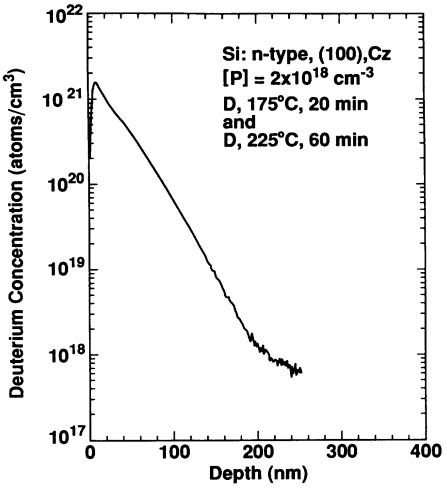

FIG. 1. Depth profile of deuterium in an NMR specimen of n-type single-crystal silicon after the following two-step deuteration treatment: (1) D, 175 °C, 20 min and (2) D, 225 °C, 60 min. The deuterium is predominantly associated with the extended planar defects that are generated by deuteration, and the deuterium profile was obtained from SIMS.

ment of about a factor of 2. The composite NMR sample, therefore, contained a SIMS-determined total of 1×10^{18} deuterium atoms that were incorporated in platelets. For the sample volume of 0.68 cm^3, this corresponds to an average deuterium density of 3×10^{18} cm^{-3} and to a deuterium to silicon ratio of 6×10^{-5} or 0.006%. This is to be compared with deuterated amorphous silicon (a-Si:D) where typically the D content is 10%. In other words, the NMR signal from our deuterated c-Si samples is expected to be some 3 orders of magnitude weaker than that from a comparable volume of a-Si:D.

Deuterium NMR measurements were performed in an external magnetic field of 8.4 T (55 MHz Larmor frequency) at temperatures from 4.2 to 40 K. A quadrupole echo pulse sequence[17] (i.e., 90°_x-τ-90°_y-τ) was used, and the resulting quadrature-detected echo at time 2τ was Fourier transformed to obtain the NMR spectrum. This pulse sequence yields the true signal (aside from a decay due to the spin-spin relaxation, T_2 decay) from spins for which the quadrupole interaction dominates. No significant signal was observed using a Hahn spin echo sequence (i.e., 90°_x-τ-180°_y-τ) which refocuses decays due to a distribution of Zeeman frequencies. This indicates that a distribution of NMR frequencies due to quadrupole interactions dominates any distribution due to magnetic interactions (e.g., chemical shifts) for the D spins. The pulse width of the 90° pulses was 7 μsec, which corresponds to a spectral width of 36 kHz. Spectral features that are split from the central resonance frequency by an amount comparable to or greater than this value are reduced in amplitude, and a known correction factor was applied to extract the true amplitude.[18] The spin-spin relaxation time, T_2, was obtained by varying τ, and the spin-lattice relaxation time, T_1, resulted from varying the repetition time. Both measurement parameters were varied over wide ranges to ensure that all of the D contributed to the signal.

The resonance frequency for D (nuclear spin 1) in a strong external magnetic field, H_0, and in the presence of an electric field gradient is

$$\upsilon=\upsilon_0\pm(\upsilon_Q/4)[3\cos^2(\theta)-1+\eta\sin^2(\theta)\cos(2\phi)]\,, \qquad (1)$$

where υ_0 is the Larmor precession frequency and υ_Q is the quadrupole frequency given by $3e^2qQ/2h$, with eq the electric field gradient, η the asymmetry in the electric field gradient, and Q the deuterium nuclear quadrupole moment. The angles θ and ϕ are the polar coordinates that specify the orientation of the principal axes of the electric field gradient with respect to the applied magnetic field. Equation (1) is valid to first order in υ_Q/υ_0, an excellent approximation in the present study with $\upsilon_0\approx55$ MHz and $\upsilon_Q\sim100$ kHz. The $\pm$ dependence arises from the two nuclear spin transitions so that Eq. (1) specifies a doublet spectrum which is centered at υ_0 and has a splitting of $\upsilon_Q/2$ times the angular expression in square brackets. The splitting, called the Pake splitting, υ_P, is readily measured as a function of angle. The dipole-dipole couplings give rise to a line broadening much smaller than υ_Q.

The D spectra for the platelet sample at 4.2 K are shown in Fig. 2 for three orientations of the sample relative to H_0. This spectrum consists of two components: a doublet described by Eq. (1) and a broad central line. We first consider the doublet. From the variation of its splitting with orientation, it is readily determined from Eq. (1)

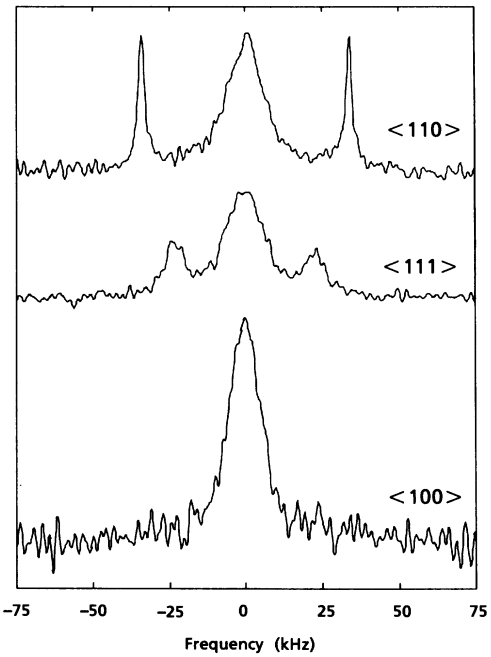

FIG. 2. The deuterium NMR spectrum for three orientations of the platelet-containing sample relative to the external magnetic field: field along the crystallographic ⟨110⟩ direction (top curve), along the ⟨111⟩ direction (middle curve), and along the ⟨100⟩ direction (bottom curve). These spectra are from the Fourier transform of the average of 100 quadrupole echos for ⟨110⟩ and ⟨111⟩ and 36 for ⟨100⟩ with $\tau=150$ μsec ($2\tau\sim T_2$) and a pulse repetition time of 50 sec ($\sim T_1$), all at 4.2 K.

that the doublet arises from deuterium nuclei that experience an electric field gradient of axial symmetry ($\eta=0$) with the principal axis along ⟨111⟩. Its magnitude is specified by $\nu_Q=136$ kHz. For example, with H_0 along ⟨100⟩, θ for the electric field gradient along ⟨111⟩ is the magic angle, 54.74°, or its complement, for which $3\cos^2(\theta)-1=0$. For $\eta=0$, no splitting occurs, as observed. Similarly, for H_0 along ⟨110⟩, $|3\cos^2(\theta)-1|=1$ and $\nu_P=\nu_Q/2=68$ kHz, as observed. For H_0 along ⟨111⟩, two doublets should be observed, one with $\nu_P=\nu_Q/3=45$ kHz and another with $\nu_P=\nu_Q=136$ kHz. Only the former is visible in Fig. 2. The latter is not observed because, from crystallographic considerations, it is smaller than the 45-kHz doublet by a factor of 2 and, more importantly, because its shift from ν_0 of 68 kHz is larger than the spectral width of the applied 90° pulses, 36 kHz. The reduction factor[18] for this line is 0.2 vs 0.9 for the 45-kHz doublet. Thus the experimental amplitude of the 136-kHz doublet is an order of magnitude smaller than that of the 45-kHz doublet and unobservable. We should comment that the width of the 45-kHz doublet is larger than that of the 68-kHz doublet because of a small misalignment of the crystal relative to H_0. Due to the geometry of the sample, the ⟨111⟩ orientation is more difficult to set than ⟨110⟩ and ⟨100⟩. A small misalignment causes a satellite line to break into several lines which can be represented as a single line broadened by about 3 kHz per degree of misalignment.

Unlike the doublet, the central line exhibits little, if any, dependence on angle. It is approximately Lorentzian in shape and has a full width at half maximum (FWHM) of 14 ± 2 kHz for both ⟨110⟩ and ⟨111⟩. The width is apparently narrower at 12 ± 2 kHz for ⟨100⟩ since the narrow doublet has collapsed onto the broad central line, creating a narrower composite line. The width of the central line is too broad to be dipolar in origin but rather is quadrupolar, consistent with its refocusing by the quadrupolar echo pulse sequence. Its larger integrated intensity shows that it contains twice as many deuterium atoms as the doublet.

Estimates of T_1 and T_2 were obtained in the ⟨110⟩ orientation. The decay of the echo, with 2τ varied from 100 to 700 μsec, is exponential and gives $T_2\approx300$ μsec for both components of the line. This corresponds to a FWHM of 1.2 kHz, due to D-D dipolar interactions. The magnetization recovery with increasing repetition time from 0.5 to 300 sec shows some nonexponential behavior and yields an average T_1 of ≈30 sec for the central line and ≈100 sec for the doublet. With the weak signals in these samples, more precise determinations of these parameters is difficult. The spectra of Fig. 2 were obtained with a pulse repetition time of 50 sec ($\sim T_1$) for optimum signal-to-noise and for $2\tau=300$ μsec ($\approx T_2$), for a reasonable tradeoff between signal intensity and distortions due to receiver recovery from the 90° pulses.

With the spectra in Fig. 2 and the determined values for T_1 and T_2, a total D spin count was obtained. D_2O diluted in water at room temperature was used as a reference. Signal intensity differences between 300 and 4.2 K were calculated and checked with deuterated amorphous silicon whose signal is readily observed at both temperatures. The NMR data for each orientation of Fig. 2 yielded a total number of deuterium atoms of $(2\pm1)\times10^{18}$, consistent with the SIMS determination.

We now consider the doublet component of the spectrum. For a D bonded to a Si dangling bond, the major component of the electric field gradient is along the bond axis and is axially symmetric about the bond axis. This is the case found for Si-D in deuterated amorphous Si where a powder pattern with $\eta=0$ and a Pake splitting of the singularities of 66 kHz ($\nu_Q=132$ kHz) is observed.[10] This corresponds well to our value of $\nu_Q=136$ kHz and a Pake splitting of 68 kHz for H_0 along ⟨110⟩. An obvious difference between the *c*-Si and the *a*-Si cases is the orientation dependence which places the Si-D bond along ⟨111⟩ in the crystalline Si. This conclusion is consistent with TEM studies that find the platelets along {111} planes. The results on the NMR doublet imply that D bonds to the Si along the surface of a platelet.

This result is consistent with a microscopic model[8] based on planar clustering of H_2^* complexes. A single H_2^* consists of a broken Si-Si bond with one H bonded at the bond-center site and a second H bonded at the antibonding site of the other Si atom. The predicted deuterium NMR spectrum for a single H_2^* is two doublets of equal intensity, both with $\eta=0$ and with a rotation pattern as observed. One doublet would have the experimentally observed $\nu_Q=136$ kHz arising from the D in the bond-center site and the other a theoretically predicted $\nu_Q\approx70$ kHz arising from the D in the antibonding site. A second doublet with a smaller splitting is not observed. So isolated H_2^*'s do not account for the doublet in the platelet sample. But as H_2^*'s cluster, the strain energy is reduced and the characteristic vibrational frequency and quadrupole coupling constant of the D in the antibonding site approach those of the bond-center site. Then the prediction of the clustered H_2^* model in the large-platelet limit is a single doublet, whose splitting and dependence on sample orientation are in agreement with our results.

The origin of the broad central line is less clear. It contains $\frac{2}{3}$ of the D in the sample and has a FWHM of 14 kHz. These parameters do not change substantially with temperature between 4.2 and 40 K; that is, no motional narrowing of the line occurs. The line is too broad to be freely rotating molecular D_2 and too narrow to be orientationally ordered para-D_2 or D in a strong Si bond. However, it is very similar to the broad central line in *a*-Si:D.[15] In the amorphous material the broad central line is independent of temperature below about 70 K but is somewhat broader (i.e., ≈25 kHz versus the 14 kHz of the present study), with some variations between samples.[15] It was originally assigned to weakly bonded D, that is, D is strained or weak bonds in the amorphous matrix. For such a bonding configuration the electric field gradient is expected to be smaller and to have a large η, resulting in a quadrupole-broadened central line as observed. More recently, an intriguing suggestion[16] has been proposed that a major part of the broad central line in *a*-Si:D is due to molecular D_2 that is trapped in the network such that its ability to translate or change rotational states is inhibited. If the transition rate between different molecular rotational states, m_J, is comparable to the intramolecular coupling

constant of 25 kHz, then a broad central line occurs. These D_2 molecules are thought to be isolated and trapped in small voids in the network. For *c*-Si both situations can be envisioned. Deuterium could be bonded in the highly strained regions around the edges of the platelets, such that the quadrupole coupling is lowered and/or is asymmetric, $\eta \neq 0$. Also molecular D_2 could be trapped in the dilated region of the platelet such that its translational and tumbling motions are inhibited; molecular D_2 would not be detected by conventional vibrational spectroscopy. A broad central line is predicted for either configuration when there is a distribution in the degree of disorder of the bonding sites and/or a distribution of platelet sizes.

This research was supported by the National Renewable Energy Laboratory (formerly SERI).

[1]N. M. Johnson, F. A. Ponce, R. A. Street, and R. J. Nemanich, Phys. Rev. B **35**, 4166 (1987).

[2]N. M. Johnson, C. Doland, F. A. Ponce, J. Walker, and G. Anderson, Physica B **170**, 3 (1991).

[3]N. M. Johnson, in *Hydrogen in Semiconductors,* edited by J. I. Pankove and N. M. Johnson (Academic, New York, 1991), Chap. 7.

[4]J. N. Heyman, J. W. Ager III, E. E. Haller, N. M. Johnson, J. Walker, and C. M. Doland, Phys. Rev. B **45**, 13363 (1992).

[5]N. M. Johnson, C. Herring, C. Doland, J. Walker, G. Anderson, and F. A. Ponce, Mater. Sci. Forum **83-87**, 33 (1992).

[6]C. G. Van de Walle, P. J. Denteneer, Y. Bar-Yam, and S. T. Pantelides, Phys. Rev. B **39**, 10791 (1989).

[7]P. Deak and L. C. Snyder, Radiat. Eff. Defects Solids **111-112**, 77 (1989).

[8]S. B. Zhang and W. B. Jackson, Phys. Rev. B **43**, 12142 (1991).

[9]P. Deak, C. R. Ortiz, L. C. Snyder, and J. W. Corbett, Physica B **170**, 223 (1991).

[10]H. P. Strunk, H. Cerna, and E. G. Mohr, Inst. Phys. Conf. Ser. **87**, Sect. 1, 457 (1987).

[11]A.-J. Jeng, G. S. Oehrlein, and G. J. Scilla, Mater. Res. Soc. Symp. Proc. **104**, 247 (1988).

[12]C. C. Tsai, G. B. Anderson, and R. Thompson, Mater. Res. Soc. Symp. Proc. **192**, 475 (1990).

[13]R. A. Street, *Hydrogenated Amorphous Silicon* (Cambridge Univ. Press, New York, 1991).

[14]A. Van Wieringen and N. Warmholtz, Physica **22**, 849 (1956).

[15]D. J. Leopold, J. B. Boyce, P. A. Fedders, and R. E. Norberg, Phys. Rev. B **26**, 6053 (1982); V. P. Bork, P. A. Fedders, D. J. Leopold, R. E. Norberg, J. B. Boyce, and J. C. Knights, *ibid.* **36**, 9351 (1987).

[16]M. P. Volz, P. Santos-Filho, M. S. Conradi, P. A. Fedders, R. E. Norberg, W. Turner, and W. Paul, Phys. Rev. Lett. **63**, 2582 (1989); P. Santos-Filho, M. P. Volz, R. L. Corey, Y. W. Kim, P. A. Fedders, R. E. Norberg, W. Turner, and W. Paul, J. Non-Cryst. Solids **114**, 235 (1989).

[17]J. H. Davis, K. R. Jeffrey, M. Bloom, M. I. Valic, and T. P. Higgs, Chem Phys. Lett. **42**, 390 (1976); N. Boden, S. M. Hanlon, Y. K. Levine, and M. Mortimer, *ibid.* **57**, 151 (1978).

[18]M. Bloom, J. H. Davis, and M. Valic, Can. J. Phys. **58**, 1510 (1980).